Analysis and Design of Steel-Concrete Composite Frame Systems

Mark D. Denavit[1], Jerome F. Hajjar[2], Roberto T. Leon[3], and Tiziano Perea[4]

[1]Design Engineer, Stanley D. Lindsey and Associates, Ltd., Atlanta, GA 30339.
[2]Professor and Chair, Department of Civil and Environmental Engineering, Northeastern University, Boston, MA 02115.
[3]Professor, Department of Civil and Environmental Engineering, Virginia Tech, Blacksburg, VA 24061.
[4]Professor, Departamento de Materiales, Universidad Autónoma Metropolitana, Mexico City, Mexico.

ABSTRACT

The lack of clear guidance regarding the value of elastic flexural rigidity (*EI*) that should be used in the analysis of steel-concrete composite columns is a significant unresolved issue that hinders the design of frame systems that include these members. The common approach of utilizing the rigidity of either the steel or the concrete only tends to be overly conservative. Other approaches that combine the rigidities have not been fully validated for use in strength and stability design procedures or for the determination of lateral deflections. To address this issue, research has been conducted to develop comprehensive recommendations for the elastic flexural rigidity of composite columns. A complimentary goal has been to validate common strength design procedures, including interaction diagrams, axial compression and bending moment anchor points, and analysis procedures to determine required strengths. In this paper, an assessment of current strength design methodologies is presented along with recommendations for potential improvements. Both the AISC Direct Analysis method and the ACI elastic second-order analysis method are investigated.

INTRODUCTION

The wide availability of structural analysis software packages that perform accurate geometric nonlinear analyses has made second-order elastic analysis design approaches very common in practice. Such design provisions exist for steel-concrete composite members in both the AISC *Specification* (AISC 2010b), as the Direct Analysis method, and the ACI *Code* (2011), as the second-order analysis method. However, neither methodology has yet been comprehensively assessed for validity and accuracy, as has been done in the past for structural steel (Kanchanalai 1977; Surovek-Maleck and White 2004) and for reinforced concrete (Hage and MacGregor 1974). This paper presents the results of a large parametric study that has been conducted to assess the current design methodologies with a particular emphasis on the elastic flexural rigidity (*EI*) recommended for analysis.

BENCHMARK FRAMES

The parametric study described in this work primarily consists of comparisons between results from second-order inelastic analyses and second-order elastic analyses on a set of benchmark frames. In order to ensure broad applicability of the recommendations, the benchmark frames are selected to cover a wide range of material and geometric properties. Similar studies for structural steel (Kanchanalai 1977; Surovek-Maleck and White 2004) have used a set of small non-redundant frames and a W8×31 section in both strong and weak axis. For this work, this set of frames was expanded and a variety of composite cross sections were selected. In the parametric study, each cross section is used within each benchmark frame to provide a comprehensive set of results.

Cross Sections

The cross sections chosen for investigation in this work are categorized into four groups 1) Circular concrete-filled steel tubes (CCFT), 2) Rectangular concrete-filled steel tubes (RCFT), 3) Steel reinforced concrete (SRC) subjected to strong axis bending, and 4) SRC subjected to weak axis bending. Within these groups, sections were selected to span practical ranges of concrete strength, steel ratio (ratio of steel cross section area to gross cross section area), and for the SRC sections, reinforcing ratio (only CFTs without longitudinal reinforcing bars are analyzed in this work). Other section properties (e.g., steel yield stress) were taken as typical values. Steel yield strengths were selected as F_y = 345 MPa (50 ksi) for W shapes, F_y = 290 MPa (42 ksi) for round HSS shapes, F_y = 317 MPa (46 ksi) for rectangular HSS shapes, and F_{yr} = 414 MPa (60 ksi) for reinforcing bars. Three concrete strengths were selected: f'_c = 27.6, 55.2, and 110.3 MPa (4, 8, and 16 ksi).

There is no prescribed upper limit of steel ratio for composite sections; however, practical considerations and the dimensions of commonly produced steel shapes impose an upper limit of approximately 25% for CFT and 12% for SRC. The AISC *Specification* (2010b) sets a lower limit of steel ratio for composite sections as 1%. However, maximum permitted width-to-thickness ratios provide a stricter limit for CFT members, corresponding to steel ratio limits of 1.86% for CCFT and 3.16% for RCFT using the steel yield strengths listed above. For SRC members, the AISC *Specification* (2010b) prescribes a minimum reinforcing ratio of 0.4% and no maximum. The ACI *Code* (2011) prescribes a maximum reinforcing ratio of 8%.

Noting these limitations, 5 round HSS shapes were selected for the CCFT sections, 5 rectangular HSS shapes were selected for the RCFT sections and outside dimensions of 711 mm × 711 mm (28 in. × 28 in.), 4 wide-flange shapes, and 3 reinforcing configurations were selected for the SRC sections (Table 1). Altogether, 5 steel shapes × 3 concrete strengths = 15 total sections were selected each for RCFTs and CCFTs and 4 steel shapes × 3 reinforcing configurations × 3 concrete strengths = 36 total sections were selected each for strong and weak axis bending of SRCs.

Frames

A set of small non-redundant frames were described and used in previous stability studies on structural steel members (Kanchanalai 1977; Surovek-Maleck and White

2004). The set includes both sidesway inhibited and sidesway uninhibited frames, a range of slenderness, end constraints, and leaning column loads. The set of frames was expanded and the frame parameters were generalized for use with composite sections in this study. The frames are shown schematically in Figure 1. The sidesway uninhibited frame is defined by a slenderness value (λ_{oe1g}), pair of end restraint parameters ($G_{g,top}$ and $G_{g,bot}$), and leaning column load ratio (γ). The sidesway inhibited frame is defined by a slenderness value (λ_{oe1g}), and end moment ratio (β). The values of these parameters selected for the frames are described in Table 2, a total of 80 frames were selected. The "*g*" in the end restraint parameters and slenderness value denotes that these values are defined with respect to gross section properties.

Table 1. Selected steel shapes and reinforcing configurations.

Index	Steel Shape	ρ_s
A	HSS 7.000×0.500	24.82%
B	HSS 10.000×0.500	17.70%
C	HSS 12.750×0.375	10.65%
D	HSS 16.000×0.250	5.72%
E	HSS 24.000×0.125†	1.93%

(a) CCFT

Index	Steel Shape	ρ_s
A	HSS 6×6×1/2	27.63%
B	HSS 9×9×1/2	19.06%
C	HSS 8×8×1/4	11.13%
D	HSS 9×9×1/8	5.05%
E	HSS 14×14×1/8†	3.27%

(b) RCFT

Index	Steel Shape	ρ_s
A	W14×311	11.66%
B	W14×233	8.74%
C	W12×120	4.49%
D	W8×31	1.16%

(c) SRC (steel shapes)

Index	Reinforcing	ρ_{sr}
A	20 #11	3.98%
B	12 #10	1.94%
C	4 #8	0.40%

(d) SRC (reinforcing configurations)

† Not a standard shape

Second-Order Elastic Analysis of Benchmark Frames

The second-order elastic results described in this work were obtained from the solution of the governing differential equation (Equation 1) using the appropriate boundary conditions. Closed form solutions were obtained for displacement and moment along the length of the column using a computer algebra system. This approach is computationally expeditious and accurate for moderate displacements; however, only flexural deformations are included. Where necessary, the effective length factor (*K*) for the benchmark frames was computed using the same differential equation.

$$v''''(x) + \frac{P}{EI} v''(x) = 0 \tag{1}$$

Second-Order Inelastic Analysis of Benchmark Frames

The second-order inelastic results described in this work were obtained from finite element analyses. Key aspects of the model are summarized here, a full description is available elsewhere (Denavit 2012). The mixed beam finite element formulation is implemented in the OpenSees framework (McKenna et al. 2000). It is a Total Lagrangian formulation assuming small strains and moderate rotations in the corotational frame and is coupled with an accurate geometric transformation. With

multiple elements along the length of a column, large displacement and rotation behavior is captured accurately.

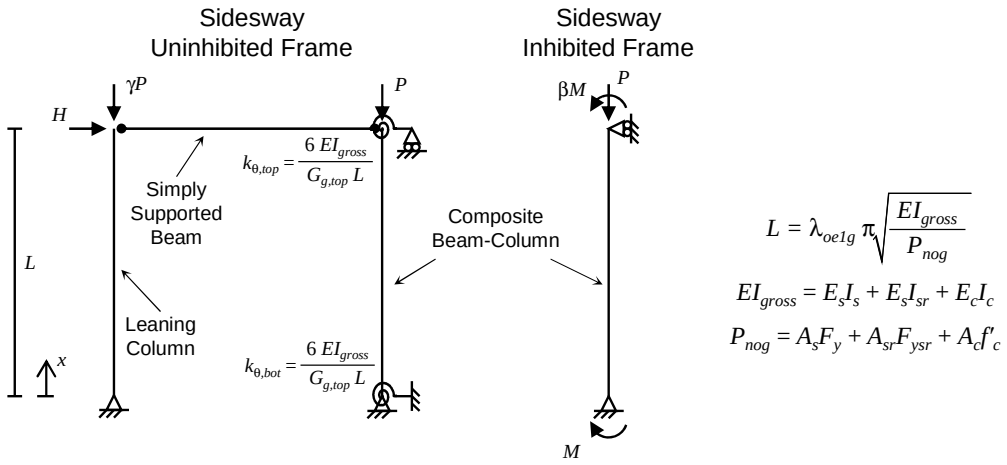

Figure 1. Schematic of the benchmark frames.

Table 2. Benchmark frame variations.

Frame	Slenderness	End Restraint	Leaning Column Load Ratio	End Moment Ratio	Number of Frames
Sidesway Uninhibited	4 values λ_{oe1g} = {0.22, 0.45, 0.67, 0.90}	4 value pairs (Table 3)	4 values γ = {0, 1, 2, 3}	n/a	64 (= 4 × 4 × 4)
Sidesway Inhibited	4 values λ_{oe1g} = {0.45, 0.90, 1.35, 1.90}	n/a	n/a	4 values β = {-0.5, 0.0, 0.5, 1.0}	16 (= 4 × 4)

Table 3. End Restraint Value Pairs.

Pair	$G_{g,top}$	$G_{g,bot}$
A	0	0
B	1 or 3†	1 or 3†
C	0	∞
D	1 or 3†	∞

†3 when γ = 0; 1 otherwise

The constitutive relations were selected to correspond to assumptions common in the development of design recommendations (e.g., neglecting steel hardening and concrete tension strength) and are comparable to those used in commensurate studies (Surovek-Maleck and White 2004). Local buckling of the steel tube and other steel components was also neglected. This simplification allows for the investigation of the full range of steel ratios without the complexity of modeling local buckling, and is consistent with the development of the Direct Analysis method for steel structures (Surovek-Maleck and White 2004).

Wide-flange shapes were modeled with elastic-perfectly plastic constitutive relations and the Lehigh residual stress pattern (Galambos and Ketter 1959). Reinforcing steel was assumed to have negligible residual stress and was also modeled with an elastic-perfectly plastic constitutive relation. Residual stresses in cold formed steel tubes

vary through thickness. To allow a reasonable fiber discretization of the CFT sections, residual stresses were included implicitly in the constitutive relation. A multilinear constitutive relation was used in which the stiffness decreases at 75% of the yield stress and again at 87.5% of the yield stress to approximate the gradual transition into plasticity observed in cold-formed steel (Abdel-Rahman and Sivakumaran 1997). In addition, the yield stress in the corner region of the rectangular members was increased to account for the additional work hardening in that region.

The Popovics concrete model was selected, with the peak compressive stress taken as f'_c or greater to account for confinement (Denavit 2012). The modulus of elasticity used in the analysis was calculated by Equation 2 taken from the ACI *Code* (2011) for normal weight concrete. Equation 2 is equivalent to the expression in the AISC *Specification* (2010b) for w_c = 2,372 kg/m^3 (148.1 lbs/ft^3).

$$E_c\left[\text{MPa}\right] = 4,733\sqrt{f'_c\left[\text{MPa}\right]} \qquad E_c\left[\text{psi}\right] = 57,000\sqrt{f'_c\left[\text{psi}\right]} \tag{2}$$

Nominal geometric imperfections equal to the fabrication and erection tolerations in the AISC *Code of Standard Practice* (AISC 2010a) were modeled explicitly. An out-of-plumbness of L/500 was included for the sidesway uninhibited frames and a half sine wave out-of-straightness with maximum amplitude of L/1000 was included for all frames. The initial out-of-plumbness and initial out-of-straightness were applied in the same direction as this produced the greatest destabilizing effect for these frames.

All frame analyses were performed with six elements along the length of the member, each with three integration points. Since the analyses were two-dimensional, strips were used for the fiber section; the nominal height of the strips was 1/30th of the section depth (e.g., for a CCFT section, approximately 30 steel and 30 concrete strips of near equal height were used). For the case of zero applied axial load, a cross section analysis was performed in lieu of the frame analysis. Often the objective of the analysis is to determine the limit point. In each analysis, the limit point was identified as the point when the lowest eigenvalue reached zero or when the maximum longitudinal strain within any section in the member reached 0.05. The strain limit was imposed since, for cases of low or zero axial load, the eigenvalue limit may not be reached or reached only at very high deformations.

AXIAL STRENGTH

In the AISC *Specification* (2010b), the nominal axial compressive strength (P_n) is determined from a column curve based on the nominal zero-length compressive strength (P_{no}) and the slenderness (λ_{oe}, Equation 3). The slenderness is a function of P_{no}, the effective length (KL) and the effective rigidity (EI_{eff}, Equation 4 for SRCs and Equation 6 for CFTs). However, when utilized within the Direct Analysis method, the nominal axial compressive strength is not necessarily representative of the maximum permitted axial load since required notional loads can impart bending moments that reduce the axial capacity. To assess the maximum permitted axial load, a second-order elastic analysis must be run to determine the applied compression force that results in internal forces the lay directly on the strength interaction diagram. An example of the beam-column interaction diagram constructed following the plastic

stress distribution approach defined in the commentary of the AISC *Specification* (2010b) is shown in Figure 2, noting that for the Direct Analysis method, the effective length factor is taken as unity.

$$\lambda_{oe} = \frac{KL}{\pi}\sqrt{\frac{P_{no}}{EI_{eff}}} \tag{3}$$

$$EI_{eff} = E_s I_s + 0.5E_s I_{sr} + C_1 E_c I_c \tag{4}$$

$$C_1 = 0.1 + 2\left(\frac{A_s}{A_c + A_s}\right) \leq 0.3 \tag{5}$$

$$EI_{eff} = E_s I_s + E_s I_{sr} + C_3 E_c I_c \tag{6}$$

$$C_3 = 0.6 + 2\left(\frac{A_s}{A_c + A_s}\right) \leq 0.9 \tag{7}$$

As prescribed in the Direct Analysis method, internal forces must be determined using a second-order elastic analysis with reduced elastic rigidity and consideration of initial imperfections. The commentary of the AISC *Specification* (2010b) recommends the reduced rigidity (EI_{DA}) be determined by applying the $0.8\tau_b$ reduction (as for structural steel) to EI_{eff} (Equation 8). The stiffness reduction τ_b depends on the required axial strength, P_r and needs adaptation since P_y, the axial yield strength, is defined only for structural steel members. For this study, P_y is taken as P_{no}, resulting in τ_b given by Equation 9.

$$EI_{DA} = 0.8\tau_b EI_{eff} \tag{8}$$

$$\tau_b = \begin{cases} 1.0 & \text{for } P_r/P_{no} \leq 0.5 \\ 4\left(P_r/P_{no}\right)\left(1 - P_r/P_{no}\right) & \text{for } P_r/P_{no} > 0.5 \end{cases} \tag{9}$$

Initial imperfections can either be directly modeled (as was done in the second-order inelastic analyses) or represented with notional loads. For the elastic analyses, the notional load approach was used. A notional lateral load equal to 0.2% of the vertical load was included in each analysis. Following section C2.2b(4) of the AISC *Specification* (2010b), the notional load was taken as a minimum load when the ratio of maximum second-order drift to maximum first-order drift was less than or equal to 1.7 and as an additive load otherwise.

Two examples of internal force point traces from elastic analyses as described above are shown in Figure 2. The frames from which the two force traces (the red and blue lines) were derived had the same cross section and column length, thus they have the same interaction diagram. The frames differed only in the stiffness of the boundary conditions and the magnitude of the leaning column load, the effects of which, for the Direct Analysis method, are expected to be captured within the analysis. The intersection of the internal force point traces and the nominal beam-column strength interaction diagram are noted as the maximum permitted axial load (P_{max}). The

intersection of the internal force point traces and the available beam-column strength (i.e., with reduction/resistance factors applied) are noted as $P_{max,\phi}$. This value is useful when comparing to strengths that have also had reduction/resistance factors applied, as will be shown later.

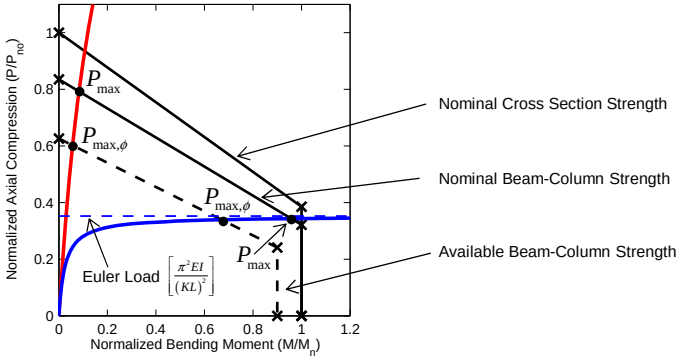

Figure 2. Schematic of interaction diagram and force trace.

The maximum permitted axial load by the elastic second order analysis approach in the ACI *Code* (2011 §10.10.4) is determined in a similar manner. A second-order elastic frame analysis is performed using a specific elastic rigidity, although no accounting of initial geometric imperfections is necessary, and the design interaction is determined following the strain compatibility method using a rectangular concrete stress distribution (ACI 2011 §10.2.7). The flexural rigidity is not explicitly given for composite sections; however, it is common to use the formula for reinforced concrete column cross sections (Equation 10). It is important to note that since the elastic analysis used in this study accounts for the geometric nonlinearity along the entire length of the column, the nonsway moment magnification procedure with its lower flexural rigidity and higher stiffness reduction was not used (ACI 2011 §10.10.2.2).

$$EI_{ACI} = 0.7E_cI_g \tag{10}$$

The critical axial load obtained from second-order inelastic analyses ($P_{analysis}$) for each section and frame pair is compared to the maximum permitted axial load from AISC ($P_{max,AISC}$) and ACI ($P_{max,ACI}$) in Figure 3. In addition to this comparison with unfactored strengths, a comparison with factored strengths is also presented in Figure 3. In the comparisons with factored strengths, $P_{analysis}$ is multiplied by a strength reduction/resistance factor (ϕ = 0.75 for the AISC methodology and for CCFTs with the ACI methodology, ϕ = 0.65 for the other sections with the ACI methodology) and $P_{max,\phi}$ is used in lieu of P_{max}. A maximum of 5% unconservative error is desired for beam-column design methodologies (ASCE 1997); this limit is shown in the figure as a red dashed line.

The results in Figure 3 show a wide range of behavior. First, the unfactored strength comparison will be examined. For CFTs by the AISC methodology, the results are generally accurate with some slight unconservative error for intermediate slenderness CCFTs and for both RCFTs and CCFTs of very high slenderness. For SRCs by the AISC methodology, for all but the stocky members, the results are very conservative, indicating that the design methodology is underpredicting the strength by a significant margin. This is due to the effective stiffness (Equation 4) and in particular the C_1

value (Equation 5) which are likely lower than necessary (Denavit 2012). The results from the ACI methodology show a wider scatter than from the AISC methodology. This is to the due use of effective rigidity for reinforced concrete cross sections (Equation 10); this equation was not intended to represent nor fully capture the benefits of the wide range of steel ratios that composite members can have. Also adding to the scatter of the ACI results is the limit that the ratio of second-order moment to first-order moment must not exceed 1.4 (ACI 2011 §10.10.2.1). This limit is a prudent measure to avoid structures that are excessively sensitive to instability, but was not accounted for in the second-order inelastic analyses.

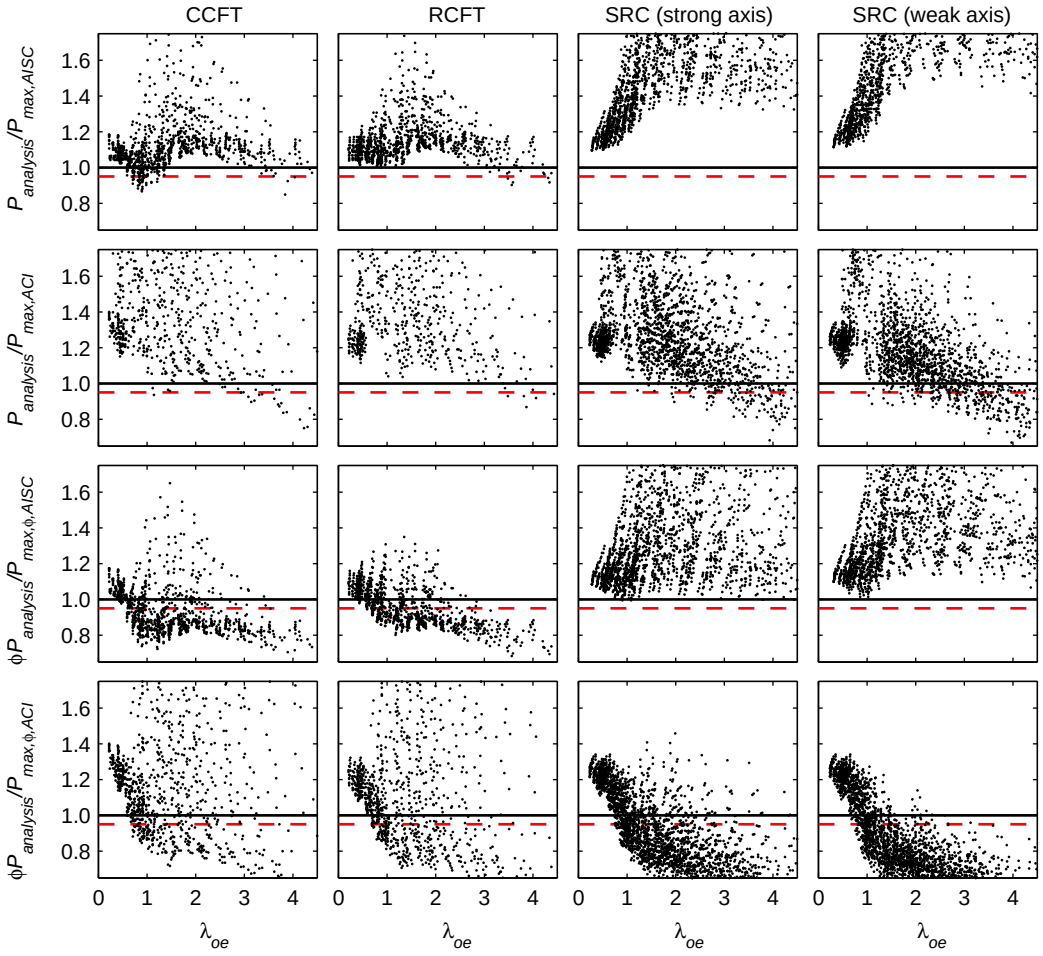

Figure 3. Axial strength results.

The factored strength comparison yields some additional insights. The factored comparison values are typically lower than the unfactored comparison values. The reason for this can be seen in Figure 2. While a constant reduction is applied to $P_{analysis}$, the difference between $P_{max,\phi}$ and P_{max} is not constant and for frames where the geometric nonlinear effects are dominant (such as the case of the blue line in Figure 2), $P_{max,\phi}$ and P_{max} can be similar in value, indicating that the strength reduction/resistance factor is not effective at reducing the strength. Both the ACI *Code* (2011) and the AISC *Specification* (2010b) recognize this and include stiffness reduction factors which are effective at reducing the strength for these cases. However, in the case of the AISC *Specification* (2010b), the stiffness reduction

recommended in the commentary (Equation 8) was developed for structural steel members and does not recognize the difference in axial compression resistance factors between structural steel and composite. For example, if τ_b was taken as 0.8 instead of Equation 9, then the total stiffness reduction would be 0.64 which is approximately equal to 0.877 times the axial compression resistance factor (0.877×0.75=0.658), commensurate with the stiffness reduction for structural steel (Surovek-Maleck and White 2004), and these errors would be negated. In the case of the ACI *Code* (2011), the flexural rigidity and stiffness reduction vary based on what methodology is used and the least favorable methodology was selected for these comparisons.

INTERACTION STRENGTH

The determination of the axial compression-bending moment interaction strength for the benchmark frames followed a similar process to that of the determination of the axial compression strength, but at several axial loads, creating interaction diagrams instead of single scalar results. In each case, a first analysis was performed to determine the axial strength as described in the previous section. A series of subsequent separate analyses were then performed applying a constant axial load and increasing lateral load until the limit point was determined.

For the inelastic analyses, both the applied loads and internal forces were recorded at the limit point, allowing for the construction of the second-order internal force interaction diagram (blue dashed lines in Figure 4 for two example benchmark frames) as well as another interaction diagram that is directly proportional to the applied loads (blue solid lines in Figure 4). The moment values in the applied load interaction diagram equal the first-order moment due to the applied loads on the frame assuming no initial geometric imperfections. The intersection of the applied load interaction diagram and the y-axis occurs at $P_{analysis}$ as defined in the previous section.

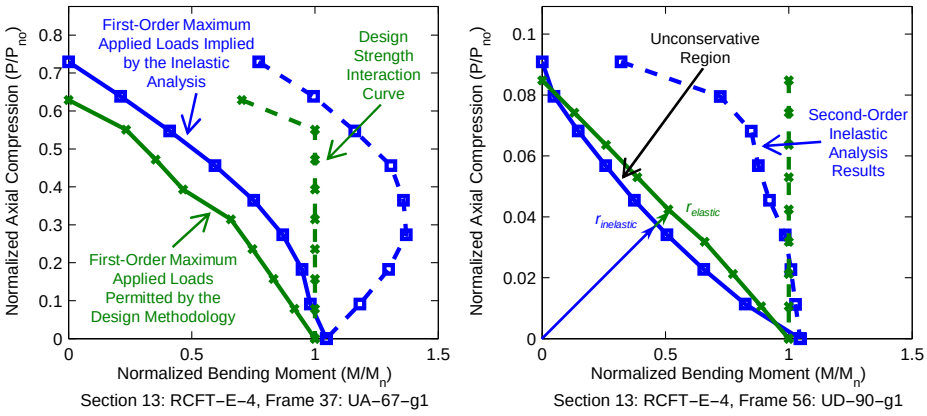

Figure 4. Comparison of interaction diagram results.

The design strength interaction diagram (i.e., calculated using either the AISC or ACI design provisions) is shown as a green dashed line in Figure 4. The green solid line in Figure 4 represents the loads that when applied in a second-order elastic analysis result in internal forces that lay directly on the design strength interaction diagram.

Just as with the inelastic results, the moment values of the solid line equal the first-order moment due to the applied loads on the frame assuming no initial geometric imperfections. The intersection of the applied load interaction diagram and the y-axis occurs at P_{max} as defined in the previous section.

In Figure 4, the green solid line indicates the envelope of applied loads that are deemed safe by the design methodology. The blue solid line indicates the envelope of applied loads that are demonstrated to be safe by the inelastic analysis. Thus, regions where the green line is outside of the blue line are considered unconservative. A radial measure is used to quantify the error (ε) is given by Equation 11, where $r_{inelastic}$ is the distance from the origin to the interaction diagram constructed from the second-order inelastic analyses (blue line) and $r_{elastic}$ is the distance along the same line to the interaction diagram constructed from the design methodology (green line). Unconservative error by this measure is represented with negative values

$$\varepsilon = \frac{r_{inelastic} - r_{elastic}}{r_{inelastic}} \tag{11}$$

Interaction strength results for RCFT cross sections are shown in Figure 5. For these results the entire suite of benchmark frames has been sorted into 30 bins based on their steel ratio and slenderness (Equation 3). For each of these bins, the maximum unconservative error in the high axial load/low bending moment range, high moment moment/low axial load range, and intermediate range has been determined and displayed. For example in Figure 5a, for benchmark frames with RCFT cross sections by the AISC methodology with steel ratio ρ_s = 0.28 and slenderness (λ_{oe}) between 2.0 and 3.0, the maximum unconservative error is 0.5% for cases of high bending moment and low axial load, 0% for cases of high axial load and low bending moment (indicating that no unconservative error was found), and 3.5% for intermediate cases. The size of the grey circles scales with the unconservative error and are shown for visualization purposes only. It is important to note that the results of Figure 5 highlight the worst-case maximum unconservative error which is useful for the following discussion, but hide the majority of cases which display no unconservative error. Also of note is that the comparisons of Figure 5 are performed at the nominal strength level, not including any reduction/resistance factors in either the inelastic analysis or elastic design methodology.

Cross section strength curves for composite members are quite convex, especially for concrete dominant members. Beam-column strength curves are much less convex (and often concave) due to the fact that material nonlinearity (primarily concrete cracking but also concrete crushing and steel yielding) initiates at low load levels and severely reduces flexural rigidity. This effect is greater for more slender columns since the second-order effects are greater but also because the ratio of bending moment to axial load is greater, a condition which leads to greater reductions in effective slenderness. This behavior has been observed experimentally (Perea et al. 2014) and is the cause of the most evident results in Figure 5, the high unconservative errors of very slender concrete dominant frames for both the AISC and ACI methodologies. This slenderness is based on the effective length (KL) so high slenderness can either be caused by long unsupported lengths (L) or by high effective

length factors (*K*) from either soft boundary conditions or high leaning column load. Also note that for the ACI methodology, the 1.4 limit on the ratio of second-order moment to first-order moment (ACI 2011 §10.10.2.1) was enforced. Likely the most effective way to reduce these errors is with modifications to the flexural rigidity used in the elastic analysis.

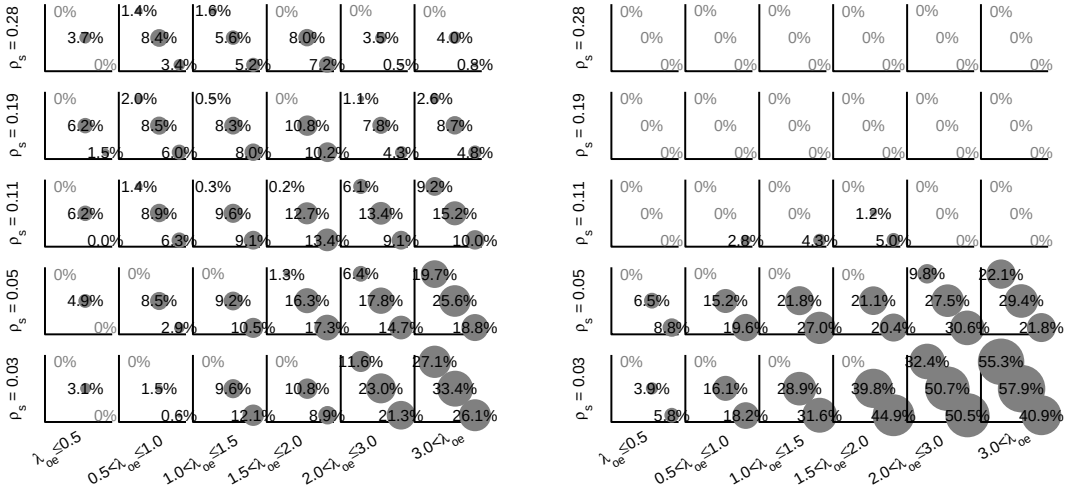

(a) RCFT cross sections – AISC methodology (b) RCFT cross sections – ACI methodology

Figure 5. Interaction strength results.

Other unconservative errors seen in Figure 5 are generally small and are typically from sidesway inhibited single curvature cases which are challenging due to the fact that cracking and the accompanying stiffness reduction will occur along the entire length of the column as opposed to just the member ends. Other section types show similar results to those seen in Figure 5 with the exception of SRCs by the AISC methodology which show little unconservative error due to the low effective flexural rigidity as discussed previously in the context of axial strengths (Denavit 2012).

CONCLUSION

A wide ranging assessment of the second-order elastic beam-column design methodologies for steel-concrete composite members in both the AISC *Specification* (2010b) and the ACI *Code* (2011) has been presented. Comparisons were made between second-order inelastic analysis results, deemed sufficiently accurate to form the basis of design recommendations, and second-order elastic analysis results, representative of the analyses an engineer performs as part of the methodology.

In general, both design methodologies were found to be safe and accurate for the majority of cases. However, some significant unconservative errors were identified, particularly for concrete dominant members with high slenderness effects and areas of potential improvement in the design provisions have been identified. The AISC Direct Analysis stiffness reduction for composite members could be revised to recognize the effects of cracking and the lower axial compression resistance factor for these members. The AISC effective rigidity for SRC members could be revised to take more full advantage of the concrete contribution. A new effective rigidity for composite columns in ACI could be beneficial to account for wide range of steel

ratios possible with these cross sections. More consistent requirements for the effective rigidity and stiffness reductions in general within the ACI *Code* (2011) could also be beneficial.

ACKNOWLEDGMENTS

This material is based upon work as part of a NEESR project supported by the National Science Foundation under Grant No. CMMI-0619047, the American Institute of Steel Construction, the Georgia Institute of Technology, and the University of Illinois at Urbana-Champaign. Any opinions, findings, and conclusions expressed in this material are those of the authors and do not necessarily reflect the views of the National Science Foundation or other sponsors.

REFERENCES

Abdel-Rahman, N., and Sivakumaran, K. S. (1997). "Material Properties Models for Analysis of Cold-Formed Steel Members." *Journal of Structural Engineering*, ASCE, 123(9), 1135–1143.

ACI. (2011). *Building Code Requirements for Structural Concrete and Commentary*. American Concrete Institute, Farmington Hills, MI.

AISC. (2010a). *Code of Standard Practice for Steel Buildings and Bridges*. American Institute of Steel Construction, Chicago, Illinois.

AISC. (2010b). *Specification for Structural Steel Buildings*. American Institute of Steel Construction, Chicago, Illinois.

ASCE. (1997). *Effective Length and Notional Load Approaches for Assessing Frame Stability: Implications for American Steel Design*. American Society of Civil Engineers, Reston, Virginia.

Denavit, M. D. (2012). "Characterization of Behavior of Steel-Concrete Composite Members and Frames with Applications for Design." Ph.D. Dissertation, University of Illinois at Urbana-Champaign, Urbana, Illinois.

Galambos, T. V., and Ketter, R. L. (1959). "Columns under Combined Bending and Thrust." *Journal of Engineering Mechanics Division*, ASCE, 85(2), 135–152.

Hage, S. E., and MacGregor, J. G. (1974). *The Second-Order Analysis of Reinforced Concrete Frames*. Structural Engineering Report No. 49, Department of Civil Engineering, University of Alberta, Edmonton, Alberta, Canada.

Kanchanalai, T. (1977). *The Design and Behavior of Beam-Columns in Unbraced Steel Frames*. CESRL Report No. 77-2, Structures Research Laboratory, Department of Civil Engineering, The University of Texas at Austin, Austin, Texas.

McKenna, F., Fenves, G. L., and Scott, M. H. (2000). *Open System for Earthquake Engineering Simulation*. Department of Civil and Environmental Engineering, University of California, Berkeley, Berkeley, California.

Perea, T., Leon, R. T., Hajjar, J. F., Denavit, M. D. (2014). "Full-Scale Tests of Slender Concrete-Filled Tubes: Interaction Behavior". *Journal of Structural Engineering*, ASCE, accepted for publication.

Surovek-Maleck, A. E., and White, D. W. (2004). "Alternative Approaches for Elastic Analysis and Design of Steel Frames. II: Verification Studies." *Journal of Structural Engineering*, ASCE, 130(8), 1197–1205.